Journal of Materials Chemistry A

ROYAL SOCIETY OF CHEMISTRY

REVIEW

View Article Online
View Journal | View Issue

Cite this: J. Mater. Chem. A, 2020, 8, 15575

A review on electrocatalytic oxidation of methane to oxygenates

Amir Hassan Bagherzadeh Mostaghimi,†[a] Tareq A. Al-Attas, †[b] Md Golam Kibria *[b] and Samira Siahrostami *[a]

Methane, the main component in natural gas, is widely utilized for energy consumption and production of important chemicals. However, existing industrial processes for (direct or indirect) production of chemicals from methane are capital-, energy-, and carbon-intensive. Alternatively, electrochemical partial oxidation of methane to high-value fuels and feedstocks is gaining momentum globally due to its modular design, adaptability with intermittent renewable energy, and operation in a wide range of temperatures and pressures. As the prices of renewable electricity continue to drop, the electrochemical pathway for methane valorization can potentially compete with century-old conventional processes if the target performance metrics can be achieved at scale. Herein, we review the recent advances in electrochemical partial oxidation of methane to high-value fuels and feedstocks, with a focus on mechanistic understanding and reaction engineering, *i.e.*, the effect of temperature, pressure, electrolyte, pH and reactor design. We conclude with some perspectives on the future development of this key research front.

Received 6th April 2020
Accepted 2nd July 2020

DOI: 10.1039/d0ta03758c

rsc.li/materials-a

1. Introduction

According to the U.S. Energy Information Administration, natural gas has the highest production growth among fossil fuels in the United States.[1] With the declining cost of natural gas due to the widespread use of hydraulic fracturing, specifically in North America, its main component, methane (92%), is gaining global traction. Apart from its traditional role in power production, cooking, and heating, it is an essential building block for synthesizing a wide range of chemicals *via* one-step or multi-step processes. For example, methane is the major feedstock for the steam methane reforming (SMR) process for industrial syngas or hydrogen production, which is an essential chemical precursor for numerous industrial processes, including Fischer–Tropsch, Haber–Bosch process, *etc.*[2] However, the SMR process involves high temperature and pressure and is energy-intensive with large amounts of associated carbon emissions. Furthermore, to reap economic benefits at scale, these processes need to operate at a large scale with a typical plant size of ~2000 to 3000 metric tons per day (MTD). Consequently, this process requires billions of dollars of capital investment and several years for commissioning. These challenges limit the application of such technologies for small-scale and highly distributed production of high-value chemicals from methane oxidation. Furthermore, it is a common practice to directly vent or flare methane from many oil and petroleum plants due to the absence of any economically viable technology to valorize methane. This leads to a vast waste of energy and negative impact on our environment, with the negative

[a]Department of Chemistry, University of Calgary, 2500 University Drive NW, Calgary, T2N 1N4, Canada. E-mail: samira.siahrostami@ucalgary.ca
[b]Department of Chemical and Petroleum Engineering, Schulich School of Engineering, University of Calgary, 2500 University Drive NW, Calgary, Alberta, T2N 1N4, Canada. E-mail: md.kibria@ucalgary.ca
† Equal contribution.

Dr Samira Siahrostami is an Assistant Professor in the Department of Chemistry at the University of Calgary, Canada. Before joining the University of Calgary, Samira was a Research Engineer (2016–2018) and a Postdoctoral Researcher (2014–2016) in the Department of Chemical Engineering at Stanford University. Prior to that she was a Postdoctoral Researcher (2011–2013) at the Technical University of Denmark. Her research focuses on modeling reactions at the surface and designing (electro)catalysts using computational methods such as density functional theory (DFT). She is a co-author of more than 60 publications in peer reviewed journals and co-inventor of two patents.

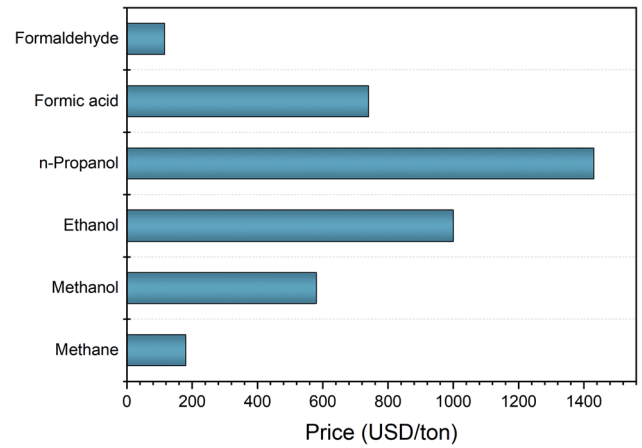

Fig. 1 Comparison of the prices of different oxygenates to that of methane in 2020.[1,4–6]

environmental impact of methane being 25 times greater than that of CO_2 over a hundred-year period. Consequently, small-scale and modular production of high-value fuels or feedstocks from methane at lower capital costs in comparison to traditional large-scale plants would be attractive to a broader range of investors, including small businesses, entrepreneurs, and project developers. Fig. 1 shows the comparison of the market prices of methane and some of the potential high-value products that could be generated from the partial oxidation of methane. Oxygenated chemicals have numerous industrial applications. For example, methanol can be converted to olefins, the building blocks of many daily basis plastic products.[3] Considering the liquid phase of the oxygenated products, these compounds can easily be transported by leveraging the existing infrastructure; thus, the challenges (*i.e.*, liquefaction cost and leakage of methane) associated with the transportation of methane or syngas could be eliminated.

However, it has been proven to be extremely difficult to partially oxidize methane to oxygenated products due to the following two reasons. Firstly, the non-polar structure of methane requires high activation energy for C–H bond dissociation (439.3 kJ mol^{-1}).[7] Secondly, once this high activation energy is provided for C–H bond dissociation, the target oxygenates, which are intermediate products, are easily activated and form thermodynamically more favorable CO_x products (Fig. 2).[8–10] Consequently, the primary step towards direct methane conversion is to seek catalysts that can selectively activate the C–H bond and prevent further oxidation to CO_x.[11]

This has motivated a lot of researchers to design processes and catalysts that facilitate the partial oxidation of methane to oxygenated products (Fig. 3). Nonetheless, most of these methods are still in their infancy and none have provided a practical pathway for partial methane oxidation to date.[12] For example, catalytic processes, which are considered the most promising approach for large scale implementation due to their direct single-step conversion feature, have shown limited efficiency and a low yield of oxygenated products.[13] On the other hand, plasma technology, which has a simple and cost-effective

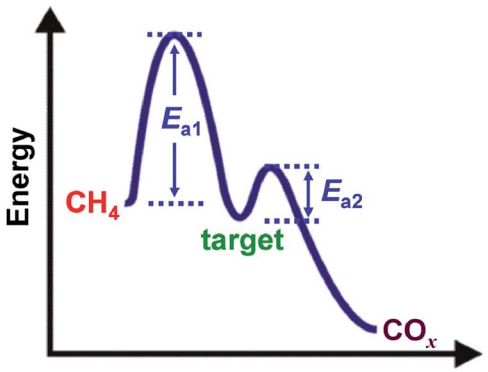

Fig. 2 Illustration of the difficulty in obtaining high selectivity towards target products. Adapted with permission from ref. 10.

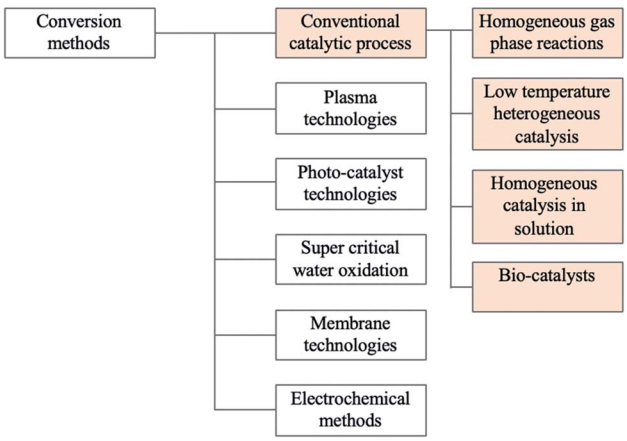

Fig. 3 Possible approaches studied in the literature for partial oxidation of methane to oxygenates.[12]

reactor design and operates under ambient conditions, suffers from low energy efficiency and lack of knowledge on surface reactions in the presence of plasma.[14–16] Supercritical water technologies have the potential to efficiently oxidize methane to oxygenated products, but selective methane oxidation to oxygenated products is limited and reactor design is complex, which hinders large scale applications.[12] Membrane technology requires high pressure to drive the reaction and efficient

Table 1 Standard electrode potential for possible methane oxidation reactions. Data are adapted from ref. 10 and 19 shown by a and b, respectively

Reaction	E (V) *vs.* RHE
$CH_4(g) + H_2O(l) \rightarrow CH_3OH + 2H^+(a) + 2e^-$	0.58[a]
$CH_4(g) + H_2O(l) \rightarrow HCHO(a) + 4H^+(a) + 4e^-$	0.46[a]
$CH_4(g) + H_2O(l) \rightarrow HCOOH(a) + 6H^+(a) + 6e^-$	0.26[a]
$CH_4(g) + H_2O(l) \rightarrow CO(g) + 6H^+(a) + 6e^-$	0.26[a]
$CH_4(g) + 2H_2O(l) \rightarrow 2CO_2(g) + 8H^+(a) + 8e^-$	0.17[a]
$2CH_4(g) \rightarrow C_2H_6(g) + 2H^+(a) + 2e^-$	0.35[a]
$2CH_4(g) \rightarrow C_2H_4(g) + 4H^+(a) + 4e^-$	0.44[a]
$2H_2O(l) \rightarrow O_2(g) + 4H^+(a) + 4e^-$	1.23[b]

Table 2 A summary of the reported studies on the electrochemical partial oxidation of methane under mild and severe conditions[a]

Reaction condition	Electrocatalyst (s)	T (°C)	P (bar)	Electrolyte	Reactor config.	Phase (s)	Oxidants	Product (s)	Ref.
Mild conditions	NiO/ZrO_2	40	1	0.1 M Na_2CO_3	Membrane electrode assembly (MEA)	Gas/liquid	O_2	CH_3OH, HCHO, CO, HCOOH, CH_3CH_2OH, CH_3COOH, CH_3COCH_3, $CH_3CHOHCH_3$	49
	$TiO_2/RuO_2/V_2O_5$	*RT	0.98	0.1 M Na_2SO_4	Single-compartment three-electrode	Liquid	H_2O	CH_3OH, HCHO, HCOOH	28
	TiO_2	20	1	1.0 M NaOH	Single-compartment three-electrode	Liquid	H_2O	CO, CO_2	63
	$PdSO_4$	140	≥6.89	Concentrated H_2SO_4	Single-compartment three-electrode	Liquid	H_2SO_4	CH_3OH	37
	ZrO_2/Co_3O_4	RT	1	0.5 M Na_2CO_3	Single-compartment three-electrode (sealed system)	Liquid	CO_3^{2-}	$CH_3CH_2CH_2OH$, $(CH_3)_2CHOH$, CH_3CHO, CH_3OH, CH_3CH_2OH	48
	$ZrO_2/NiCo_2O_4$	RT	1	0.5 M Na_2CO_3	Single-compartment three-electrode (sealed system)	Liquid	CO_3^{2-}	$CH_3CH_2CH_2OH$, $CH_3CH(OH)CH_3$, CH_3CH_2COOH, CH_3COCH_3, CH_3COOH	54
	Pt	RT	High-pressure	1 mM $K_2Pt^{II}Cl_4$ with 10 mM NaCl	Two-compartment three-electrode	Liquid	Pt^{IV}	CH_3OH, CH_3Cl, $CH_2(OH)_2$, HCOOH, CO_2	21
	TiO_2/RuO_2	RT	0.98	0.1 M Na_2SO_4	Single-compartment three-electrode	Liquid	H_2O	CH_3OH, HCHO, HCOOH	58
	Hg/Cu	RT	1	2 M KOH	Two-compartment three-electrode	Liquid	O_2	CH_2O, CH_3OH, CO, CO_2	64
	NiO/ZrO_2	RT	1	0.1 M Na_2CO_3	Membrane electrode assembly (MEA)	Gas/liquid	O_2	CH_3OH	65
	Mo/MCM-22 (zeolite)	710	1	$BaZr_{0.7}Ce_{0.2}Y_{0.1}O_{3-\delta}$ (BZCY72)	Co-ionic membrane (both proton and oxide)	Gas	O_2	C_2, C_6H_6, C_7H_8, $C_{10}H_8$, CO	86
Harsh conditions	Pd Au/C	≥50	0.5	$Sn_{0.9}In_{0.1}O_7$	SOFC	Gas	O_2	CH_3OH, CO_2	29
	V_2O_5/SnO_2	100	0.1	$Sn_{0.9}In_{0.1}P_2O_7$	SOFC	Gas	O_2	CH_3OH, CO_2	27
	$Sr_2Fe_{1.5}Mo_{0.5}O_{6-\delta}$ (SFMO)	800–900	1	$La_{0.9}Sr_{0.1}Ga_{0.8}Mg_{0.2}O_{3-\delta}$ (LSGM)	SOEC	Gas	H_2O	C_2H_4, C_2H_6, CH_4, CO, H_2	71
	$(La_{0.8}Sr_{0.2})_{0.95}MnO_{3-\delta}$ (LSM)	800	1	$La_{0.9}Sr_{0.1}Ga_{0.8}Mg_{0.2}O_{3-\delta}$ (LSGM)	SOEC	Gas	O_2	CO, H_2	72
	Ni/YSZ (yttrium stabilised zirconia)	700–1000	1	$La_{0.8}Sr_{0.2}MnO_3$ (LSM)	SOFC	Gas	O_2	CO, H_2	73
	$Sr_2Fe_{1.5}Mo_{0.5}O_{6-\delta}$–$Ce_{0.8}Sm_{0.2}O_{1.9}$ (SFM–SDC)	750–850	1	$La_{0.9}Sr_{0.1}Ga_{0.8}Mg_{0.2}O_{3-\delta}$ (LSGM)	SOEC	Gas	H_2O	CO, H_2	74
	Ni/YSZ	≥800	1	YSZ	SOFE	Gas	O_2	CO, H_2	75
	$Ni/BaZr_{0.1}Ce_{0.7}Y_{0.1}Yb_{0.1}O_{3-\delta}$ (BZCYYb)	500	1	$Ce_{0.8}Sm_{0.2}O_2$ (SDC)	SOFE	Gas	H_2O	CO, H_2	62

[a] *RT: room temperature.

membranes are costly.[12,17] Photocatalytic processes are potentially attractive methods to activate methane due to their simplicity and ease of operation.[11] In this method, the energy required for methane activation can be obtained under mild conditions by photochemical reactions where, ultraviolet and visible light provide the required energy to form electrons and holes on the surface of the photocatalyst. These electrons and holes subsequently form electrophilic oxygen species that can dissociate the C–H bond in methane.[11,12] The majority of reported products in photocatalytic methane oxidation gas-phase systems are H_2, CO_2, and C_2H_6. The formation of C_2H_6 is a result of non-oxidative coupling of methyl radicals generated at the surface of the photocatalyst. The partially oxygenated products such as methanol are not dominant in a solution-based system due to overoxidation by highly active oxygen species generated on the photocatalyst surface. Therefore, a highly selective and efficient photocatalyst to satisfy the industrial demand is yet to be developed.[11]

Overall, although these technologies have brought new dimensions to partial oxidation of methane to oxygenates, they remain in their infancy and distant from commercialization. Future directions must focus on ways to increase the selectivity and product yield for easy scale-up of small-scale distributed plants.

With the continuous drop in renewable electricity price, electrochemical processes have emerged as a promising alternative for partial oxidation of methane to oxygenates. Considering their modular design, the electrochemical routes offer a facile decentralized process that can be implemented for highly distributed small to large scale applications to directly convert methane to valuable oxygenates. The electrochemical process can efficiently utilize intermittent renewable energy to significantly reduce the emission and store intermittent energy in chemical bonds for daily to seasonal energy storage. Hence, it represents a more sustainable route to produce oxygenates under mild reaction conditions. Moreover, the selectivity and the activity of the electrocatalyst can be adjusted and controlled simply by changing the voltage. However, despite many attempts, the reported activity, selectivity, and current density for partial electrochemical oxidation of methane remain low and distant from the values needed for commercialization.[10,18] Due to the close proximity of the electrode potentials of various products, selective production of oxygenates is challenging, which negatively affects the downstream separation cost. Table 1 shows the possible oxidation reactions along with their redox potentials. It is obvious that CO_2 formation will be the bottleneck for partial oxidation of methane owing to its low redox potential.

This review summarizes different reports in the literature on the partial electrochemical oxidation of methane to determine the parameters contributing to product yield and selectivity (Table 2). This understanding sheds light on the path to take for developing more efficient catalyst materials and reactors for methane oxidation to value-added chemicals. We note that there are very limited experimental and theoretical reports and as a result there is a lack of thorough fundamental understanding in this emerging research front. In the following sections, we summarize these existing reports by focusing on two different aspects; mechanistic understanding and reaction engineering. Fig. 4 presents a timeline for the progress in the field of methane electrooxidation processes. Throughout this review, different aspects of these reports will be discussed.

2. Mechanistic insight into electrochemical methane oxidation

Electrochemical oxidation of methane could follow several different pathways resulting in different products (Fig. 5). Oxygenates such as alcohol and formaldehyde are obviously the target chemical products with high economic values (Fig. 1).

Although several experimental studies have been reported in the last few decades for electrochemical oxidation of methane, a limited number of computational reports exist to provide a clear understanding of the reaction mechanism. Platinum is

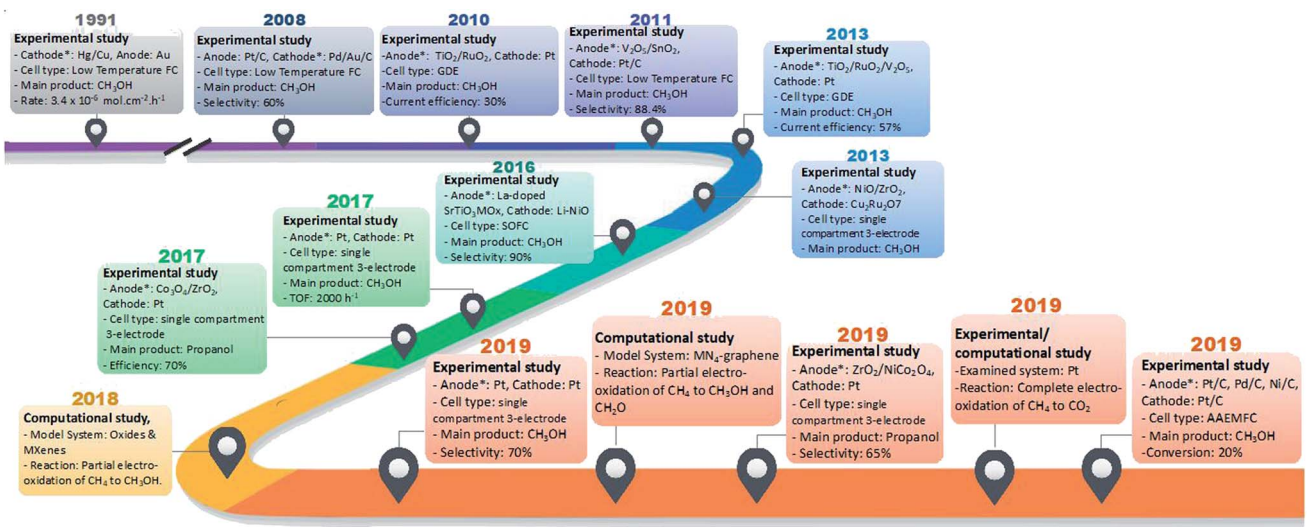

Fig. 4 Timeline for the emergence of different reports on partial electrochemical oxidation of methane to oxygenated products.

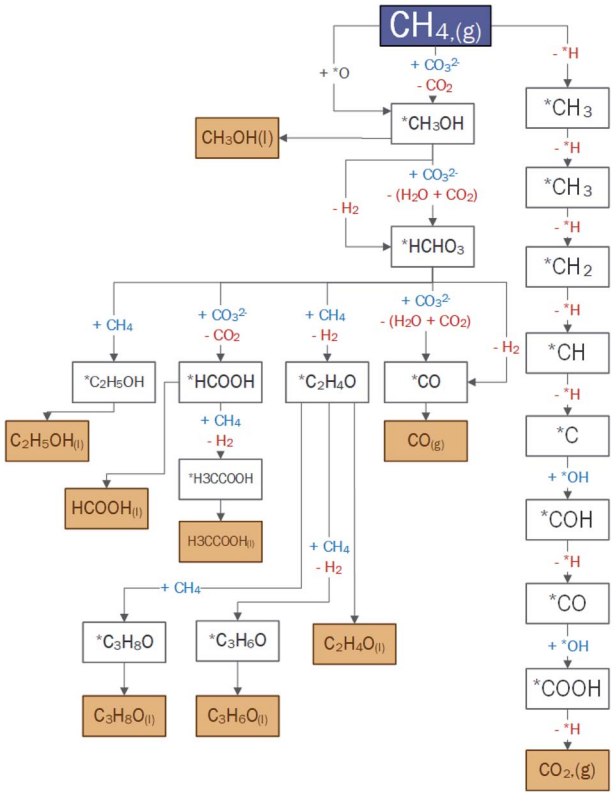

Fig. 5 Proposed pathways for electrocatalytic oxidation of methane to oxygenated products.

the most studied catalyst material for complete electrochemical oxidation of methane to CO_2 (Table 1).[11,20–22] A combined computational and experimental study by Boyd *et al.*,[23] on a Pt surface provided an improved understanding of the reaction mechanism and the factors determining catalytic activity and selectivity. Although the focus of this work is not on partial oxidation of methane to oxygenates, the results can be used to understand why selectivity is an issue for Pt and other transition metals. Using density functional theory calculations and experiments, they showed that the rate-determining step is the activation of methane with minimal dependence on the applied potential. CO was predicted to be the most stable intermediate on the Pt surface (Fig. 6), and a scaling relationship between the activation energy of methane and CO adsorption energy was established for several transition metals. This analysis showed that transition metal surfaces with strong CO adsorption energy have lower energy barriers for CH_4 activation, which could increase the overall reaction rate. However, strong adsorption of CO to the surface causes poisoning of active sites and results in low reaction rate. To avoid poisoning and increase the rate of the experiment, they increased the applied potential which resulted in favoring CO_2 formation. This analysis further elaborated that breaking the scaling relationship between methane activation and CO adsorption energy is the key to successfully producing oxygenated products.

Other experimental and computational studies in the literature have proposed reaction mechanisms for the electrochemical oxidation of methane to oxygenates such as methanol and formaldehyde. These reports can be classified into four different categories depending on the type of oxygen source and the proposed mechanism, which are discussed in the following sections. Fig. 7 summarizes the different oxygen sources as well as the catalyst used in each system.

2.1 Surface oxygen species

As listed in Table 1, electrochemical oxidation of methane involves water. Both methane oxidation and water oxidation take place at the anode of the electrochemical cell. Water oxidation results in the formation of active oxygen species at the catalyst surface (R1 and R2).

$$H_2O(l) + * \rightarrow OH* + (H^+ + e^-) \quad (R1)$$

$$OH* \rightarrow O* + (H^+ + e^-) \quad (R2)$$

A recent computational study by Arnarson *et al.*[19] shows that the presence of oxygenated species at the surface of the catalyst improves the facile hydrogen abstraction from methane and increases the rate of methane oxidation. They examined (110) surfaces of rutile transition metal oxides and monolayer MXenes using DFT calculations and showed that the catalyst

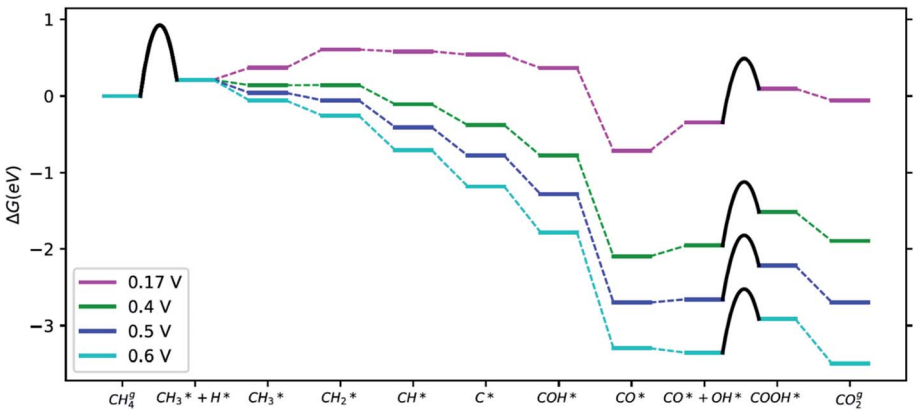

Fig. 6 Free energy diagram for complete electrochemical oxidation of methane to CO_2, adapted from ref. 23.

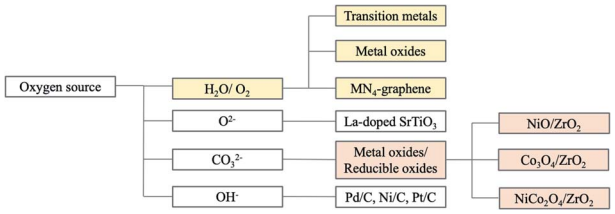

Fig. 7 Various oxygen sources investigated for partial electro-oxidation of methane to oxygenated products including electrocatalysts used.

materials on which electrochemical water splitting is a bottleneck, present a low rate for the methane oxidation reaction. Fig. 8a shows the OER activity volcano where the catalyst materials located at the left leg of this volcano are suitable for methane oxidation due to the ease of formation of adsorbed oxygen (O*). They further calculated the rate of methane oxidation, taking into account the O* availability and showed that the energy barrier for methanol formation decreases by increasing the applied potential (Fig. 8b). As a result, the rate of methanol formation increases at a given temperature. They also investigated the rate of methanol production *versus* OER as a function of the O* binding energy (Fig. 8c) and showed that by increasing the electrode potential, the OER is facilitated, and abundant active oxygen species are formed at the surface. This results in the formation of O_2 as the main product and a decrease in the rate of methanol formation. Therefore, although OER intermediates can provide the necessary active oxygen species for the reaction to proceed, they can also act as a competing reaction at higher potentials. A desirable catalyst must be able to preserve OER intermediates even at the high potentials to increase the methane oxidation rate.

In another computational study, Luo *et al.*[24] examined a variety of metal porphyrins (MN_4) (M = Cr, Mn, Fe, Co, Ru, Rh, Os, and Ir) embedded in graphene for catalyzing electrochemical oxidation of methane to light alkanes and methanol. This class of material has been reported to be active OER catalysts in previous studies.[25,26] Therefore they can be employed for the generation of essential surface oxygen to

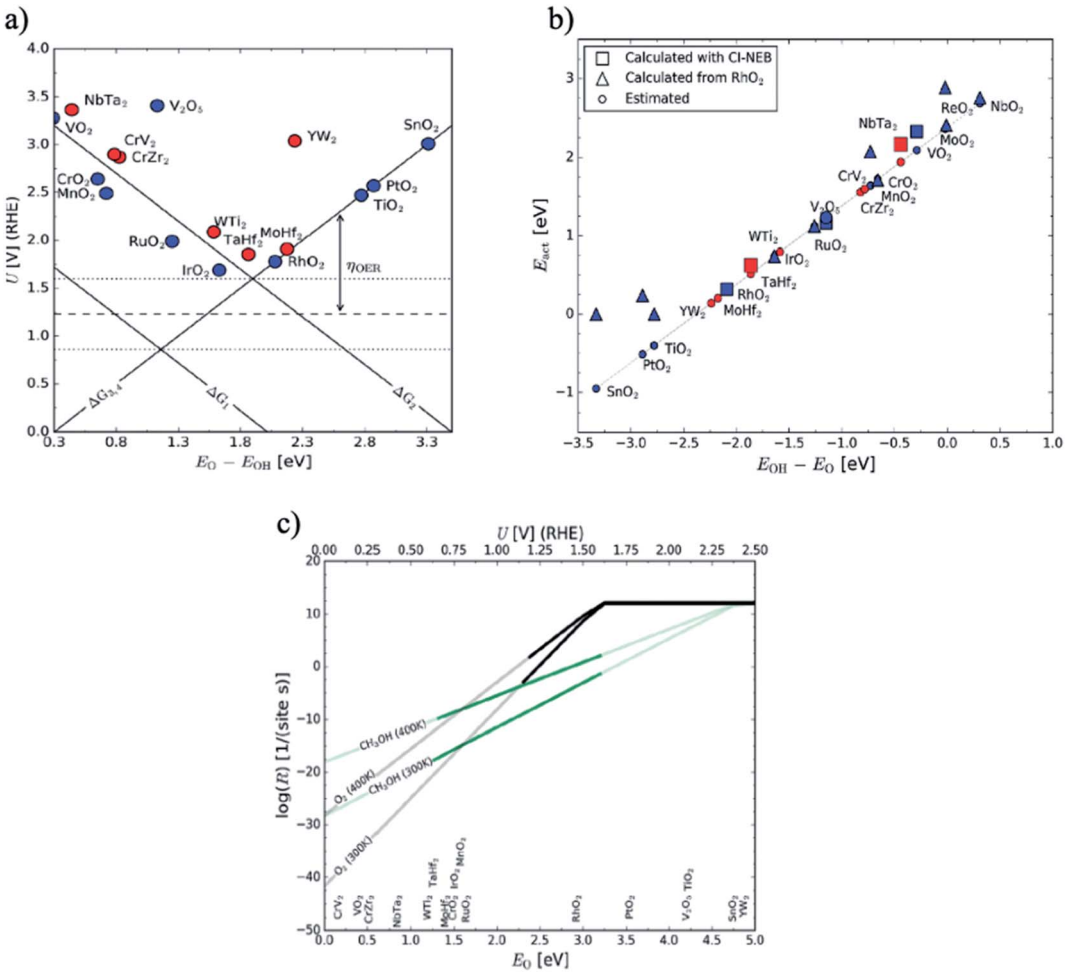

Fig. 8 (a) Activity volcano plot for the water oxidation reaction. Blue and red circles show the results for rutile transition metal oxides and MXenes, respectively. (b) Activation barrier for methane activation *versus* the descriptor $E_{OH} - E_O$. Blue points represent metal oxides, and red points stand for MXenes. (c) The reaction rates for the OER (black line) and methane oxidation (green line) are plotted at different temperatures as a function of E_O and potential. Figures are adapted with permission from Ref. 19.

activate methane. The other advantage of these materials is that the active metal centers are isolated which would limit the access to active oxygens and prevent over oxidation of methane. The authors also constructed a pourbaix diagram which is a useful tool to study coverage of active oxygens and oxygenated products at pH between 0 and 14 and a potential of 0 to 2.5 V. This analysis showed that continuous oxygenated product formation requires a careful pH and potential control and even small changes in potential or pH prevent the oxidation process or cause overoxidation of the products. Finally, FeN_4 and IrN_4 were predicted to be active for production of formaldehyde and methanol, respectively.

Experimental studies are more abundant than computational studies in the field of electrochemical oxidation of methane to oxygenates. In 2011, Hibino *et al.* investigated transition metal oxide catalysts with particular emphasis on V_2O_5.[27] They first used Pt/C as a catalyst for anodes in a temperature range of 50 to 250 °C. They reported no electrochemical oxidation of methane to oxygenates under the open circuit conditions even at high temperatures. After electrochemical reactions, the products generated on the anode side were examined, and it turned out to be O_2 and CO_2. As mentioned above, overoxidation of methane on the Pt surface also reported in ref. 23 can be attributed to the strong CO adsorption energy and subsequent CO_2 formation (Fig. 6). Therefore, instead of pure metal catalysts, the authors explored metal oxides. To improve the reaction yield towards methanol, they examined different metal oxide catalysts and supports (Mn_2O_3/WO_3, CrO/SnO_2, and CoO/V_2O_5) and showed that methanol selectivity is increased to 50% over V_2O_5 supported on SnO_2. The XPS analysis of the catalyst shows the formation of the V^{5+}/V^{4+} redox couple on the SnO_2 support, which can be the potential active site for methanol formation. These results indicated that the formation of active oxygen species is necessary to drive the reaction. V_2O_5 has also been reported in another study by Rocha *et al.*,[28] as an active electrocatalyst for methane oxidation. They showed that addition of 5.6% V_2O_5 to a TiO_2/RuO_2 electrocatalyst doubles the current efficiency to 57% at 2.0 V. This report will be further reviewed in Section 3.4. Therefore, V_2O_5 appears to be a promising electrocatalyst for partial oxidation of methane. The computational study by Arnarson *et al.* suggests that defects and low coordinated sites in V_2O_5 are the active sites.[19]

The role of active surface oxygen species in both the anode and cathode of the electrochemical cell has been reported in a previous experimental report by Hibino *et al.* where they used a proton exchange membrane fuel cell to oxidize methane to methanol (selectivity ~6.03%) at the cathode made of Pd–Au/C.[29] They explained that the surface-active oxygen species (*O) formed by the ORR reaction at the cathode surface promote methane activation and methanol formation. In a follow-up study in 2010,[30] they repeated the reaction at the anode side by adding Cu to the Pd–Au/C electrocatalyst. They also used a micro-electrochemical reactor and sprayed the catalyst on the proton exchange membrane. Their results showed that by feeding a mixture of O_2, H_2O, and CH_4 to the cell, Cu increases the yield of methanol. The obtained selectivity towards methanol formation in this cell type was 100%, however, the yield was only 0.003%. Although more information is needed to study the effect of Cu for such enhancement, the results signify the effect of cell configuration on the selectivity of methanol formation.

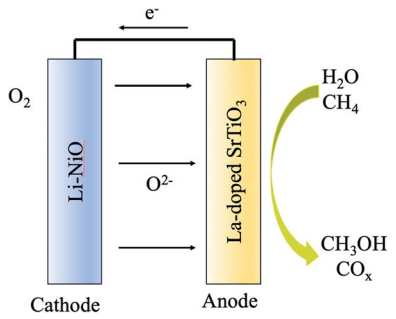

Fig. 9 Solid oxide fuel cell used for electrochemical oxidation of methane. In this cell, oxygen is reduced at the cathode side and conducted to the anode in a temperature range of 300–600 °C.

2.2 Oxygen ions

As discussed in Section 2.1, the formation of active oxygen species on the surface of the electrode where methane oxidation takes place could result in facilitating the competing reactions and ultimately decreasing the selectivity. In this section, we discuss the proposed ways in the literature to tackle this issue by producing active oxygen species at the cathode and transferring them through an ion conductive membrane to the anode for C–H bond activation. This can be achieved by utilizing solid oxide fuel cells (SOFCs) at temperatures higher than 600 °C. SOFCs are based on the reduction of an O_2 molecule on the cathode side and diffusion of the generated O^{2-} ions through an ion conductive solid oxide electrolyte to the anode.[31,32] Fig. 9 schematically shows this idea using a study by Torabi *et al.*[33] where they used NiO and Li-doped $SrTiO_3$ perovskite as the cathode and anode of a SOFC, respectively in a temperature range of 300 °C to 600 °C.

In this study they reached a methanol selectivity of more than 90% and demonstrated that the presence of oxygen ions (O^{2-}) enhances C–H bond activation for selective production of oxygenates. They suggested that lattice oxygens (O^{2-}) are able to selectively oxidize methane to methanol whereas intermediate oxygens (at the catalyst surface) will cause overoxidation. Since lattice oxygens are responsible for selective oxidation of methane, the rate of the reaction is mainly governed by the rate of transferring intermediate oxygen (*O) to lattice oxygen (O^{2-}). Since this approach does not rely on the OER reaction to form active oxygen species, the rate of oxygen accessibility is not limited by competing reactions.

2.3 Redox couples

In the mechanisms mentioned above, the presence of an active oxygen species is essential for the C–H bond dissociation. However, it is possible to activate methane using metal redox couples in an acidic medium in a temperature range between

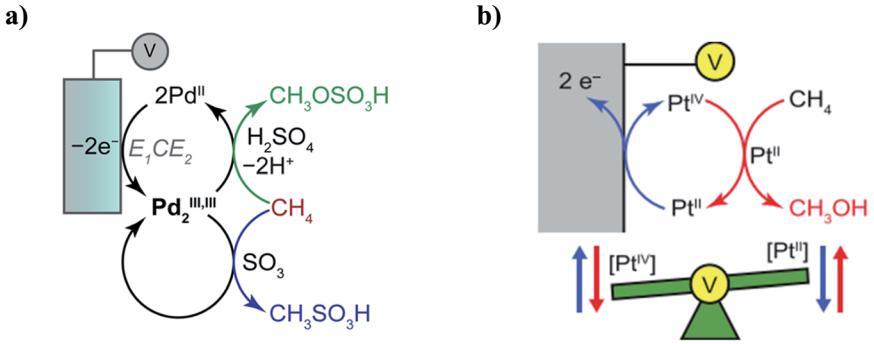

Fig. 10 (a) The 2e⁻ redox cycle of methane oxidation. The resultant CH_3OSO_3H and CH_3SO_3H species will hydrolyze to generate methanol. (b) Electrochemical formation of methanol by the $Pt^{II/IV}$ redox couple. Reproduced with permission from ref. 21 and 37.

100 °C and 450 °C.[34–36] This method has the advantage to eliminate the presence of active surface oxygens. Surendarnath *et al.*[37] used electrophilic high-valent metal ions such as Pd^{III} for the oxidation of methane to methanol in a concentrated H_2SO_4 solution and high methane pressure (Fig. 10a).

In this examined system, a methanol precursor (CH_3SO_3H) is rapidly formed by electrochemical activation of methane on $Pd^{II}SO_4$ in strong sulfuric acid. Since this system does not provide active oxygen species, continuous generation of high valent metal ions to activate the C–H bond plays a significant role in product formation. Under anodic polarization, Pd^{II} is re-oxidized to generate $Pd_2^{III,III}$ species that can activate methane. The reported turnover frequency for methane functionalization was as high as 2300 h^{-1} at 140 °C. The only drawback of this process is that separation of the product from the solution with a strong acid is challenging.

To tackle the problem with reliance on a strong acid, in a follow-up study, the oxidizing agent was switched to Pt^{IV}.[21] In this study, a Pt electrode was used to oxidize Pt^{II} to Pt^{IV} (Fig. 10b) where Pt^{IV} species form Pt^{IV}–CH_3, and then were hydrolyzed to release the oxygenated product, *i.e.*, methanol. As Pt is known for full oxidation of methane to CO_2, it is essential to protect the produced methanol from further oxidation. To tackle this issue the authors introduced chlorine ions to the reaction chamber to avoid further oxidation and to regenerate the $Pt^{II/IV}$ redox couple.

2.4 Other oxygen sources

In thermal and photochemical oxidation of methane to methanol, H_2O_2 and NO_2^- have been broadly used as oxygen sources.[38–45] However, electrochemical oxidation of methane to oxygenated products has not been thoroughly explored, and the reports on other oxygen sources are limited to the application of carbonate (CO_3^{2-}) and hydroxyl ions (OH^-).[46–48]

Spinner *et al.*[49] reported the formation of CH_3OH, HCHO, CO, and $HCOO^-$ at room temperature using CO_3^{2-}. Carbonate ions were conducted through an ion conductive electrolyte to the anode side where methane oxidation occurs. Negatively charged oxygen coming from CO_3^{2-} was suggested to activate the C–H bond. The catalyst reported in this study was a mixture of NiO and ZrO_2 with NiO being used for methane activation[50] and ZrO_2 for facilitating the adsorption of CO_3^{2-}.[51–53]

In a similar setup, by Ma *et al.*[48] ZrO_2 nanoparticles were adsorbed on the surface of Co_3O_4 plates. The ion-conducting electrolyte was removed and Na_2CO_3 was added to the solution as the source of CO_3^{2-}. This method provided faster kinetics since CO_3^{2-} ions were already in the electrolyte and trapped on the ZrO_2 surface. The surface of Co_3O_4 was used for methane activation. The catalytic superiority of Co_3O_4 to NiO_2 was confirmed by electrochemical performance analysis. However, Co_3O_4 was not able to oxidize methane to oxygenated products and it turned out that the presence of ZrO_2 was necessary. This work demonstrated fast and mild oxidation of methane to oxygenated products such as 1-propanol and 2-propanol with a product efficiency of around 60%. A follow up study in 2019 investigated replacing Co_3O_4 with $NiCo_2O_4$. The product efficiency in this study was reported to be 60% under ambient conditions. The high catalytic activity was attributed to the reducible property of $NiCo_2O_4$. Reducible oxides are highly affected by the reversible oxidation state of the metals. Due to this property, these types of materials can store and release oxygen species from their lattice structures.[55] The Co–O bond is relatively weak which makes it possible to form oxygen vacancies even at low temperatures. The excess electrons resulting from the absence of oxygen can be redistributed on empty cation sites. This phenomenon increases the lattice oxygen mobility and enhances catalytic activity for oxidation reactions.[54,56]

Hydroxyl radicals have also been used as an oxygen source for partial electrochemical oxidation of methane using alkaline anion exchange membrane fuel cells (AAEMFCs) and an ion conductive membrane to carry OH^- ions from the cathode to anode.[57] Santos *et al.*[47] reported 20% methane conversion with methanol and formate products using an AAEMFC with Pt/C, Pd/C, and Ni/C as anode materials at room temperature. To identify the reaction path and product stability, infra-red (IR) measurements were performed during the reaction. The results for the Pt/C surface indicated that methanol formation commences at the OCP (~0.3 V), and the methanol bands disappear as the potential approaches 0.0 V, which can be attributed to the overoxidation of methanol to COO species. On

the Pd/C surface, however, methanol bands exist at all potentials, although they become quite small around zero potential. Methane oxidation to COO products was observed even at OCP on Ni/C with little variation during potential change. This result indicates that Ni/C is able to activate methane with no applied potential.

3. Reaction engineering

Apart from the electrode material and controlling the oxygen source, several other variables can affect partial electrochemical oxidation of methane and the ultimate reaction product. In this section, we overview studies in the literature based on electrolyte engineering, temperature, pressure, and electrolyzer configuration. Addressing such parameters have a significant impact on energy efficiency and product selectivity of the electrochemical methane oxidation reaction. This section summarizes the guidelines from the literature for optimizing the cell design through tuning the reaction environment as well as electrode/electrolyte architecture.

3.1 Electrolyte engineering

Although there are several studies based on the use of solid-state electrolytes, ionic liquids, and organic electrolytes, electrochemical oxidation of methane has mostly been examined in aqueous electrolytes. The presence of liquid electrolyte plays a significant role in liquid-phase electrolyzers for facilitating ion transfer and providing a reaction environment. The kinetics of methane electrocatalysis at the electrode/electrolyte interface can be controlled by altering the pH. Electrochemical oxidation of methane has been demonstrated in alkaline, neutral, and acidic media. Methane has extremely poor solubility in aqueous solutions (>22.7 mg L^{-1}), which hinders its conversion in the conventional electrocatalytic systems carried out in acidic, alkaline or neutral media.[11,12,58] A study by Santos *et al.*[47] shows the successful conversion of methane to methanol (~20% at 0.3 V cell voltage) on a Pt/C electrocatalyst using an alkaline anion-exchange membrane fuel cell (AAEMFC). This enhancement was attributed to the suppression of proton availability in the vicinity of the reaction interface in the alkaline medium, which facilitates the production of methanol.

Amenomiya *et al.*[50] showed that OH^- has negligible activity in abstracting a proton from methane under mild conditions. As mentioned in the previous section, methane could be oxidized using a charged oxygen atom in CO_3^{2-}-based electrolytes. This results in improving oxidation kinetics and increasing reaction enthalpy.[49,59,60] Therefore, CO_3^{2-}-based electrolytes result in overall better performance than OH^--based electrolytes for alkaline-based systems.[48,49,54] Moreover, metal oxide catalysts reported for methane oxidation, *e.g.*, NiO,[49] Co_3O_4,[48] and $NiCO_2O_4$,[54] are more stable under alkaline conditions.

Acidic media were reported for the catalytic cycle of methane oxidation using Pt[21] and Pd[37] salts and is shown to stabilize catalyst ions during the catalytic cycle.[21] Kim *et al.*[21] employed the Shilov catalytic system by deploying aqueous Pt salts ($Pt^{II/IV}$) in concentrated acid media (0.5 M H_2SO_4) to avert the stoichiometric use of the expensive Pt^{IV} oxidant.[61] This approach led to a steady methane oxidation catalysis with 70% selectivity for methanol *via* maintaining the $Pt^{II/IV}$ ratio during the Pt^{II}-catalyzed methane oxidation cycle.

3.2 Temperature

Temperature is another determining factor in the electrochemical methane oxidation process. Due to the high activation energy required for C–H bond activation in methane, the kinetics of direct electrochemical oxidation under mild conditions is extremely sluggish.[48,62] Nevertheless, partial electrochemical oxidation of methane to oxygenates has been vastly studied at room temperature in liquid-phase electrolytes,[21,28,48,54,58,63–65] where an electrochemical cell with solid electrodes is commonly used and methane is dissolved in the liquid phase. We show herein that combined temperature, and potential control could enhance partial electrochemical oxidation of methane, through different effects such as increasing anion/cation mobility, local methane activation, and metal/oxide interface interactions.

Hibino *et al.*[27] investigated the effect of temperature on electrochemical methane oxidation to methanol using a confined fuel cell-type reactor. The reaction was first conducted over a Pt/C anode fed with a mixture of methane and water vapor at temperatures between 50 and 250 °C. As the temperature increased, the concentration of methane decreased, and the current density increased. However, the major products were O_2 and CO_2, with a higher temperature lowering the O_2 and increasing the CO_2 concentration. As discussed in Section 2.1, they investigated several non-platinum catalysts and non-carbon supports for methanol production, where V_2O_5/SnO_2 showed the most significant results. At 100 °C, the faradaic efficiency for methanol production was 61.4%. Moreover, chronopotentiometry results revealed that the highest methanol production is obtained at potentials around +900 mV. Using several characterization techniques such as TEM, XRD, and XPS they concluded that the vanadium species were partially reduced and highly dispersed on the SnO_2 support. They showed that methane is oxidized to methanol using the active oxygen species generated by the anodic polarization of water vapor over V^{4+} sites at potentials around +900 mV.

High-temperature oxygen-ion conducting solid oxide anodes have shown significant promise for partial electrochemical oxidation of methane to carbon monoxide with typical operating temperatures higher than 500 °C.[66–70] Oxygen-ion conducting solid oxides have generally been studied for electrochemical steam reforming of methane.[27,29,62,71–75] The electrode resistance dramatically decreases as the operating temperature is increased. Thus, increasing the operating temperature would significantly lower the cathode polarization associated with the reduction of oxygen.[62] The rate of ionic transport and catalytic activity can be dramatically improved by carefully designing suitable nanostructured electrodes.[76] The main drawback of implementing oxygen-ion-conducting solid oxide electrolytes is the high activation energy (E_a) associated with oxygen-ion

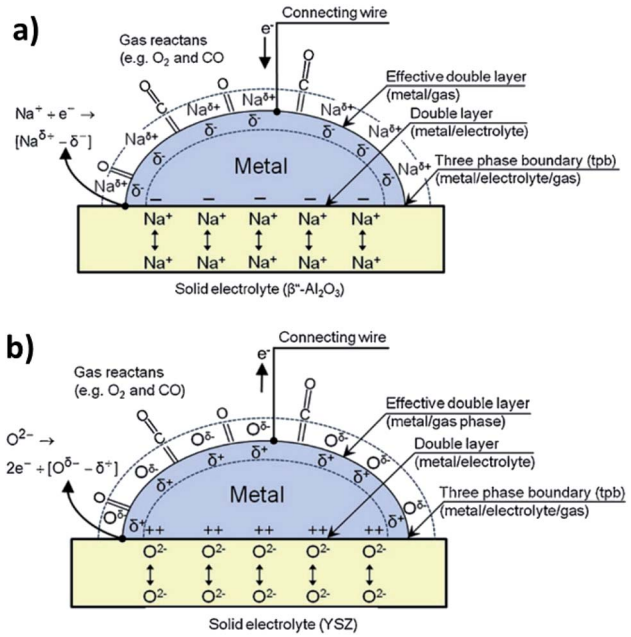

Fig. 11 Schematic diagram of a metal electrode deposited on (a) Na-β′ – Al_2O_3, a Na^+ conductor and (b) YSZ, an O^{2-} conductor, showing the location three-phase boundary (tpb). The classical double layer is located at the metal-support interface, while the effective double layer is located at the metal–gas interface. Reproduced with permission from ref. 83.

conduction. Alternatively, proton conduction in oxides generally has lower E_a compared to oxygen-ion-conduction.[77–81] Hence, protonic ceramic cells offer an appealing potential for attaining high-performance at lower temperatures. Proton ceramic electrolytic cells show better performance for resisting coke formation while being used for hydrocarbon fuels. This advantage is due to the direct removal of protons, which disfavors the undesired Boudouard reaction at the anode.[81] A study by Duan *et al.*[81] suggested using a protonic ceramic electrolyte for a fuel cell, which lowered the required operating temperatures to 250–550 °C from ≥600 °C associated with its solid oxide counterpart. The reaction was used for power generation in which methane was completely oxidized to CO_2.

The metal/oxide interface, which can be formed after the *in situ* growth of metal nanoparticles on a host oxide lattice, improves both redox and long-term stability by avoiding particle agglomeration caused by the reduction of surface energy. Lu *et al.*[72] showed that the stiff metal/oxide interface enhances the chemical activation of CO_2 and hinders the coke formation during the electrochemical reforming of CH_4/CO_2 to produce syngas. A similar conclusion was reported by Zhu *et al.*[71] in which the *in situ*-grown metal/oxide interface hindered coking and enhanced the catalyst stability at high temperatures for the electrochemical oxidation of CH_4 to C_2H_4 in an oxide-ion conducting solid oxide electrolyte. Moreover, the metal/oxide interfaces at the nanoscale would accommodate oxygen species of O^- ions that are required during the transformation of O^{2-} ions to the active interfaces at the anode. These active oxygen species also work on activating CH_4; however, the electrochemical pumping of O^{2-} ions from the cathode to the anode would directly oxidize methane in conjunction with gaseous selective coupling to produce C_2H_4 in the presence of suitable interface catalysts.

A study by Zagoraios *et al.* exploited the electrochemical double layer located at the metal–gas interface for methane oxidation at temperatures up to 460 °C.[82] Fig. 11 shows the difference between the classical double layer and the effective double layer present in a Na^+ conductor and an O^{2-} conductor. This phenomenon is termed the Electrochemical Promotion of Catalysis (EPOC), also known as the Non-Faradaic Electrochemical Modification of Catalytic Activity (NEMCA) effect. The EPOC effect can be used to boost the conductivity of metal or metal–oxide catalytic films deposited on solid electrolytes. The approach can be explained *via* the formation of an effective overall neutral double layer created by applying an electrical current (or potential) on the catalytic surface. In this study, the anode was the Pd/Co_3O_4 composite powder deposited on an yttria-stabilized zirconia (YSZ) solid electrolyte. The results indicate that presence of the effective double-layer increased the

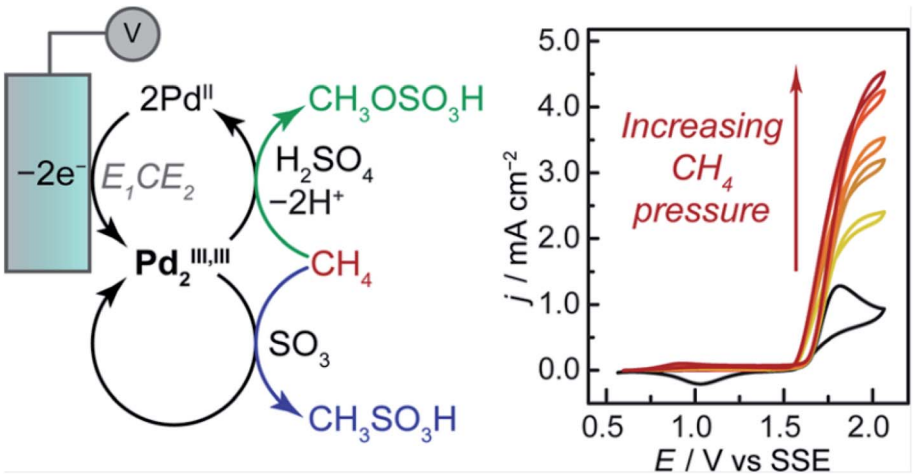

Fig. 12 The effect of increasing CH_4 pressure (0 to 500 psi) on functionalization by an electrogenerated $Pd_2^{III,III}$ species. CVs (20 mV s^{-1} scan rate) of $PdSO_4$ (~23 mM) in concentrated H_2SO_4. Reproduced with permission from ref. 37.

catalytic rate for Pd/Co_3O_4 coated on YSZ by 2.5-fold compared to a Pd film electrode supported on YSZ. While only CO_2 and H_2O were observed as methane combustion products, the knowledge gained from the EPOC approach can be implemented for future studies on high-temperature partial electrochemical methane oxidation.

3.3 Pressure

The pressure of methane is another important factor that could affect both electrolytic performance and integration between up- and downstream operations. The main benefit of elevated pressure is to enhance methane solubility in an aqueous system, which allows for higher oxidation current densities. Moreover, tuning the partial and absolute pressure of methane affects product selectivity by altering the relative surface coverage, and binding energies of adsorbed oxidants and methane oxidation intermediates.[84] Nevertheless, there have been a few studies that introduced pressurized systems for partial electrochemical oxidation of methane.[21,37] O'Reilly *et al.*,[37] reported selective electrophilic methane mono functionalization—generating methanol precursors *i.e.*, methyl bisulfate (CH_3OSO_3H) and methane sulfonic acid

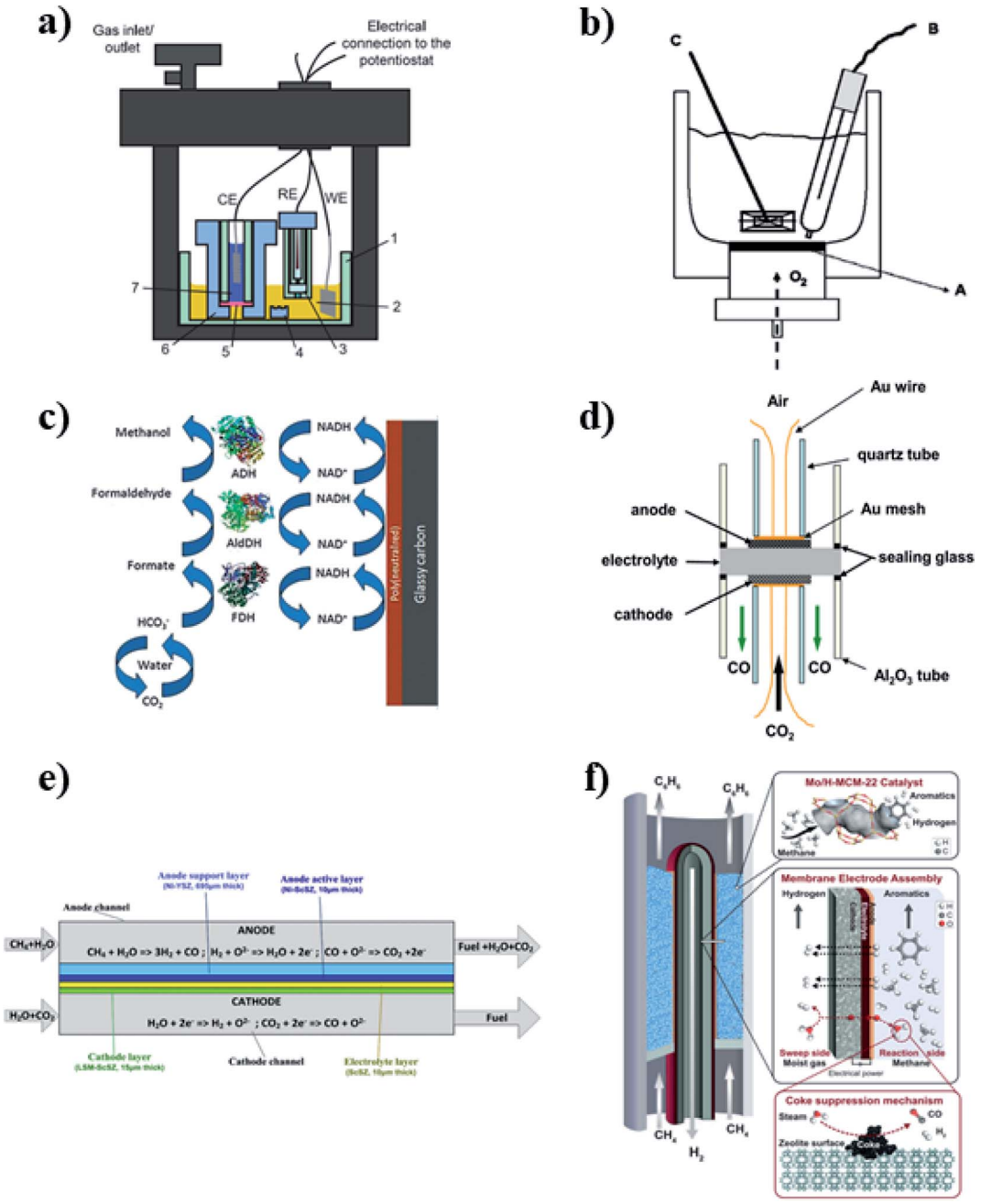

Fig. 13 Electrochemical cell configurations used for partial methane oxidation under mild and severe conditions. (a) Single compartment two/three-electrode liquid cell; (b) gas-diffusion electrode gas per liquid cell; (c) glassy carbon electrode, and severe conditions; (d) button cell; (e) channel cell; (f) co-ionic cell. Reproduced with permission from ref. 21, 85–87.

(CH_3SO_3H)—*via* electrochemical oxidation of simple Pd^{II} salts in concentrated sulfuric acid solutions at 140 °C (Fig. 12). Pressurizing the electrochemical cell with 100 psi of methane raised the anodic peak at 1.82 V to higher current densities all the way up to 500 psi. Lowering the reaction temperature to 100 °C showed the same behavior of direct proportionality of pressure with current density. However, the anodic current, beyond 1.5 V, became less pronounced due to the weakening of the $Pd_2^{III,III}$ back-reduction peak, which implies utilization of the high-valent species during methane oxidation.

3.4 Electrolyzer configurations

Electrolyzer configuration used for methane oxidation could significantly affect the overall performance. Fig. 13 summarizes the electrochemical cell configurations suggested in the literature for partial oxidation of methane at ambient and high temperatures. Since the electrochemical oxidation of methane is still in its early stage, the main focus has been on catalyst development and optimization through performance testing using liquid phase two-electrode electrolyzers using a modified glassy carbon electrode (Fig. 13c).[23,54,60] A sealed three-electrode system was also tested to let the reaction occur for a couple of hours.[48,54] Departing from traditional liquid electrolyzer configurations, several studies have applied solid oxide electrolyzer configuration that has the advantage to be operated in continuous mode delivering desirable conversion rates and selectivities.[71,72]

The limited solubility of methane restricts achieving high conversions with elevated current densities. Therefore, Ma *et al.*[48,54] suggested running long-term electrochemical oxidation of methane in a closed two-electrode system at room temperature. The electrolyte was bubbled before the electrochemical reaction with methane for 1.5 h to remove dissolved oxygen and to fill the vacant space in the cell. Methane was maintained in the gas phase to make sure the consumed methane in aqueous electrolytes would be compensated by dissolving in the electrolyte continually. The electrochemical oxidation was conducted at 2.0 V *versus* Pt for up to 20 hours. Their results showed that increasing the reaction time increases the production rate of propionic acid and acetone by further oxidizing intermediate products, *i.e.*, 1-propanol, 2-propanol, and acetaldehyde. Methane conversion was 47.5% after 20 hours.

Although non-polar organic solvents, *e.g.*, cyclohexane, benzene, and toluene, increase methane solubility in liquid electrolytes, these electrolytes are more prone to be oxidized than methane. Hence, introducing a gas diffusion electrode (GDE) with a porous structure could highly enhance the electrolytic oxidation of methane by having a triple-phase boundary of gas–liquid–solid. The accommodation of the GDE can improve the overall performance by eliminating the mass transport limitation associated with the poor solubility of methane. Rocha *et al.*,[28,58] investigated the use of GDE configuration for methane oxidation (Fig. 13b). They adopted the same cell design that was previously reported for oxygen reduction to hydrogen peroxide with a carbon/PTFE gas

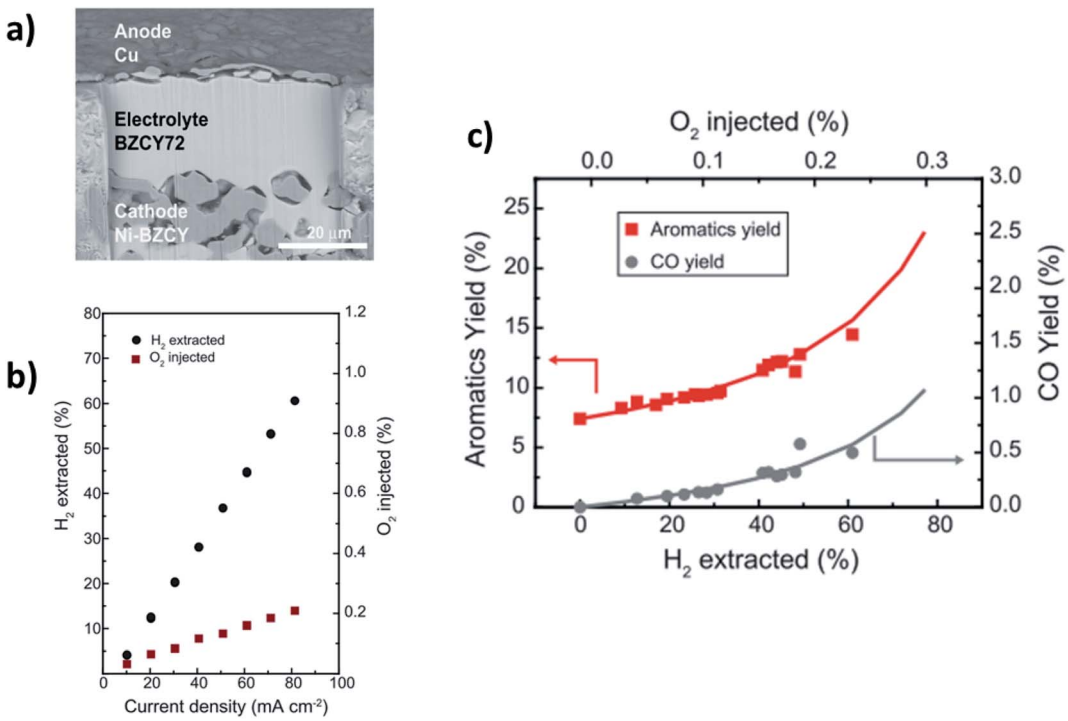

Fig. 14 (a) Scanning electron microscopy (SEM) image of the co-ionic membrane electrode. (b) Percentage of O_2 injected and H_2 extracted current density at 700 °C. The cathode is swept with a 3/5/92 mixture of $H_2O/H_2/Ar$, while the anode is swept with a mixture of 10/90 H_2/CH_4. (c) CO and aromatics yield as a function of O_2 injected and H_2 extracted at 700 °C and 1 bar. Reproduced with permission from ref. 86.

diffusion electrode,[85] consisting of mixed $TiO_2/RuO_2/V_2O_5$. In this study, an optimum amount of V_2O_5, *i.e.*, 5.6%, doubled the total faradaic efficiency to 57% at 2.0 V *vs.* SCE. They concluded that adopting a GDE to continuously feed the cell with methane increases selectivity for methanol even at low current densities.

High-temperature solid oxide electrolysis cells (SOECs) have great potential for efficient and economical partial oxidation of methane by integrating thermal catalysis and electrocatalysis, which facilitates methane oxidation even at ambient pressure. Unlike conventional thermo-catalytic methane oxidation processes, the introduction of electricity would allow the process to be operated at ambient pressure and provide a driving force for shifting the reaction equilibrium toward the desired product. High-temperature SOECs, including reversible fuel cells,[88] dry methane fuel cells,[62] methane/carbon dioxide reforming,[72] nonoxidative methane dehydroaromatization,[86] and methane oxidation to ethylene have been reported with reasonable performance characteristics.[71] The button cell configuration is the most commonly reported SOEC configuration.[62,71–75,81,89] In this configuration, the solid electrolyte is sandwiched between a porous anode and a porous cathode (Fig. 13d). In practice, button cells could be designed to be stacked on top of each other to improve the overall cell performance. The stack button cell assembly generally consists of circular cells that are interconnected with commercial ferritic stainless steel. The temperature gradient is reduced inside a furnace before entering the stack by preheating both the fuel stream and the air stream.

Morejudo *et al.*[86] adapted a co-ionic membrane reactor in which both protons (H^+) and oxide ions (O^{2-}) are conducted through the solid electrolyte (Fig. 13f). The electrolyte of the membrane is composed of acceptor doped $BaZrO_3$. At elevated temperatures, this doped electrolyte features an ability to take up protons from steam and exhibiting high conductivity for both protons and oxide ions.[90] The electrochemical co-ionic membrane was exploited to achieve the nonoxidative methane dehydroaromatization (MDA: $6CH_4 \leftrightarrow C_6H_6 + 9H_2$) using shape-selective Mo/zeolite. Fig. 14a shows a scanning electron microscopy image of the tubular membrane, which consists of a dense 25 mm-thick $BaZr_{0.7}Ce_{0.2}Y_{0.1}O_{3-\delta}$ (BZCY72) electrolyte film coated on top of a porous BZCY72-Ni support. Ni acts as a cathode, which has sufficient catalytic activity for the reduction of steam and H_2 evolution. A Cu-based anode was implemented on the electrolyte film to promote electrochemical oxidation of H_2 (H_2 extraction) to protons to suppress the undesired coke formation. Both hydrogen extraction from the cathode and injection of oxide ions through the membrane to the anode increased proportionally with increasing the current density at 700 °C (Fig. 14b). Furthermore, increasing the magnitude of the imposed co-ionic current increased the aromatics yield, which surpassed the theoretical equilibrium yield, *i.e.*, 12.3%. This elevated performance is due to the *in situ* H_2 extraction that shifts the equilibrium towards aromatics formation. The CO formation also increased parallel to the aromatics yield with increasing co-ionic currents (Fig. 14c). They concluded that the use of an electrochemical co-ionic membrane reactor improves the techno-economic process viability, where high carbon efficiencies can be achieved (up to 80%).

The use of SOECs was further studied using Multiphysics modeling by Xu *et al.*[87] They numerically investigated methane assisted co-electrolysis of CO_2 and H_2O using a 2D model in a micro-scale tubular SOEC model that couples the process of electrochemical reactions in porous electrodes, ionic/electronic charge transport in electrolyte and electrodes, chemical reactions in channels and porous electrodes, momentum transport in channels and micro-pores and mass transport in channels and micro-pores (Fig. 13e). The model reveals that this system substantially lowers the electrical power consumption for the co-electrolysis of H_2O/CO_2 by reducing the equilibrium potential of the SOEC (Fig. 15a). Moreover, increasing the reaction temperature considerably increases the performance of

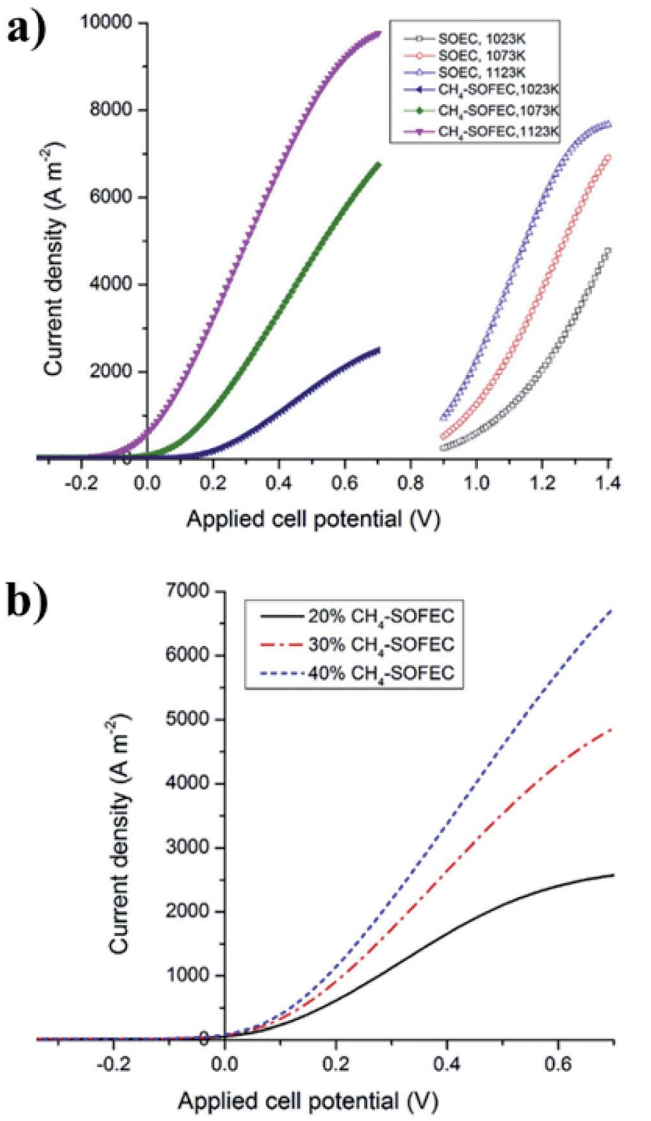

Fig. 15 (a) Temperature effect of CH_4-SOFEC and SOFC co-electrolysis at 0.7 V and 1.4 V for the CH_4-SOFEC and SOEC, respectively. (b) Performance of the CH_4-SOFEC at 1073 K at different inlet methane mole fractions. Reproduced with permission from ref. 87.

methane-assisted SOECs (CH_4-SOFEC). This behavior was attributed to boosting reaction kinetics of both electrochemical reactions and methane reforming reactions (Fig. 15b). The optimum yield of the proposed setup was at 1123 K, with a current density of 600 A m^{-2}.

4. Summary and perspectives

Continuous price reduction of renewable electricity and natural gas opens a tremendous opportunity for electrochemical partial oxidation of methane to high-value oxygenated products. In contrast to the conventional energy, capital, and carbon-intensive methane conversion technologies (*i.e.*, steam methane reforming), electrochemical oxidation offers intermittent, modular, as well as operation in a wide range of temperatures and pressures for highly distributed production of oxygenated products. Unfortunately, effort in this key research front is still lacking, and the technology is still in its infancy and distant from commercialization.

Due to the high activation energy required for C–H bond dissociation, selective and partial electro-oxidation of methane is thermodynamically and kinetically challenging, and the fundamental understanding of the reaction pathway is yet to be established. The computational studies using DFT calculations have revealed that the binding energy of the reaction intermediates is related to the C–H activation barrier. This relationship has been used to estimate the catalytic activity and explain, for example, why V_2O_5 is selective for methanol production or Pt is active for complete oxidation of methane to CO_2. Combined computational and experimental results show that the oxygen source plays a major role in methane activation and reaction product selectivity. Oxygen ions and lattice oxygen atoms are also reported to result in more efficient electrochemical conversion of methane. Therefore, the employed electrocatalyst must efficiently produce and deliver these active oxygen species. This point can be used as a guideline for designing efficient electrocatalysts. Throughout this contribution we showed some of the most successful reports that ensure the presence of active oxygens at a variety of catalyst surfaces. These examples mostly include metal oxides and particularly reducible oxides which have high lattice oxygen mobility and are considered as potential candidates for electro-oxidation of methane to value added products. However, further experimental and computational studies are required to carefully examine other catalytic systems and unravel the effect of different oxygen sources such as hydroxyl or peroxyl.

Moreover, it is worth mentioning that partial electro-oxidation of methane is a multiscale problem. Although the catalyst material and design of active sites are very important, the various reports in the literature summarized in this review paper provide good evidence on the importance of reaction conditions and electrochemical cell design. The situation is very much similar to the CO_2 reduction reaction (CO_2RR) which is comparatively a more mature research field. The research in this field has shown that even a good catalyst such as copper is not efficient without a proper cell design and reaction conditions and a proper selection of the electrochemical cell, electrolyte and reaction conditions is the key to control the selectivity and activity. The less number of publications in the field of partial electro-oxidation of methane makes it difficult to draw a comprehensive conclusion. However, positive actions have been taken and there are several reports showing that selectivity and activity can be controlled by reaction conditions such as temperature, pressure, electrode, electrolyte, pH, cations, anions and cell design for similar types of catalyst material. Moreover, understanding the nature of the double layer on the electrode–electrolyte interface would allow tackling the most appropriate reaction environment. Taking this into consideration, there is a lot of room for improvement in partial electrochemical oxidation of methane to oxygenates.

We highlight several key challenges that need to be addressed to achieve breakthroughs in this field. The first is the lack of mechanistic understanding of possible reaction pathways at a molecular level, due to the limited number of studies dedicated to partial electrochemical oxidation of methane compared to the more studied complete oxidation of methane. *In situ* spectro-electrochemical studies combined with computational modeling would accelerate addressing this issue. Second, the lack of standard reporting protocols, which often results in false-positive and irreproducible findings appearing in the literature, misleads the researchers and restrains follow-up studies. Third, the electrolytic methane conversion must be accomplished at industrially relevant current densities, *i.e.*, >300 mA cm^{-2}, a necessary condition for industrial applicability. Therefore, rigorous benchmarking protocols (methane purification, isotopic labeling and multiple control experiments) are required to detect and quantify the oxidation products and to enable faster development of this key research front towards practical application. This can be addressed by departing from traditional H-type cell configuration and implementing liquid/gas-phase electrolyzers, such as liquid electrolyzer gas diffusion electrodes and membrane assembly electrodes. Furthermore, although methane electro-oxidation at a high temperature is well studied using an oxygen-ion conducting electrolyte, research should be directed towards proton-conducting electrolytes, which require lower operating temperatures compared to their solid oxide counterpart.

In the thermochemical oxidation of methane, highly uniform metal clusters, in particular Cu–oxo, are reported to be highly active towards partial oxidation of methane. It is generally accepted that incorporation of these clusters into MOFs or enzymes would generate highly active catalytically active sites that can selectively oxidize methane.[91,92] Despite their outstanding activity towards the partial oxidation of methane, the electrocatalytic performance of these materials is not well studied and the nature of active sites in electrocatalysts for partial oxidation of methane is yet to be explored.

Lastly, we are confident that there are many promising economic and environmental advantages of the selective electrochemical oxidation of methane to oxygenated products. Due to the daily increasing market demand for chemical oxygenates and concerns about climate change, competitive alternatives for currently used industrial methods are necessary and require a high amount of research as well as innovative approaches.

Conflicts of interest

There are no conflicts to declare.

Acknowledgements

The authors gratefully acknowledge the support from the University of Calgary's Canada First Research Excellence Fund Program, the Global Research Initiative in Sustainable Low Carbon Unconventional Resources.

References

1 U.S. Energy Information Administration (EIA), https://www.eia.gov/.
2 M. A. Peña, J. P. Gómez and J. L. G. Fierro, *Appl. Catal., A*, 1996, **144**, 7–57.
3 U. Olsbye, S. Svelle, M. Bjørgen, P. Beato, T. V. W. Janssens, F. Joensen, S. Bordiga and K. P. Lillerud, *Angew. Chem., Int. Ed.*, 2012, **51**, 5810–5831.
4 Q. Lu and F. Jiao, *Nano Energy*, 2016, **29**, 439–456.
5 Independent Chemical Information Services (ICIS), https://www.icis.com/explore/.
6 M. Jouny, W. Luc and F. Jiao, *Ind. Eng. Chem. Res.*, 2018, **57**, 2165–2177.
7 P. Schwach, X. Pan and X. Bao, *Chem. Rev.*, 2017, **117**, 8497–8520.
8 M. O. Adebajo, *Green Chem.*, 2007, **9**, 526–539.
9 P. Tang, Q. Zhu, Z. Wu and D. Ma, *Energy Environ. Sci.*, 2014, **7**, 2580–2591.
10 S. Xie, S. Lin, Q. Zhang, Z. Tian and Y. Wang, *J. Energy Chem.*, 2018, **27**, 1629–1636.
11 X. Meng, X. Cui, N. P. Rajan, L. Yu, D. Deng and X. Bao, *Chem*, 2019, 1–30.
12 Z. Zakaria and S. K. Kamarudin, *Renewable Sustainable Energy Rev.*, 2016, **65**, 250–261.
13 P. Khirsariya and R. K. Mewada, *Procedia Eng.*, 2013, **51**, 409–415.
14 B. Lemmens, H. Elslander, I. Vanderreydt, K. Peys, L. Diels, M. Oosterlinck and M. Joos, *Waste Management*, 2007, **27**, 1562–1569.
15 T. Nozaki, A. Aĝiral, S. Yuzawa, J. G. E. Han Gardeniers and K. Okazaki, *Chem. Eng. J.*, 2011, **166**, 288–293.
16 S. Liu, L. R. Winter and J. G. Chen, *ACS Catal.*, 2020, **10**, 2855–2871.
17 C. Duan, M. Luo and X. Xing, *Bioresour. Technol.*, 2011, **102**, 7349–7353.
18 J. Jang, K. Shen and C. G. Morales-Guio, *Joule*, 2019, **3**, 2589–2593.
19 L. Arnarson, P. S. Schmidt, M. Pandey, A. Bagger, K. S. Thygesen, I. E. L. Stephens and J. Rossmeisl, *Phys. Chem. Chem. Phys.*, 2018, **20**, 11152–11159.
20 F. F. Tao, J. J. Shan, L. Nguyen, Z. Wang, S. Zhang, L. Zhang, Z. Wu, W. Huang, S. Zeng and P. Hu, *Nat. Commun.*, 2015, **6**, 7798.
21 R. S. Kim and Y. Surendranath, *ACS Cent. Sci.*, 2019, **5**, 1179–1186.
22 Q. Huang, W. Li, Q. Lin, X. Zheng, H. Pan, D. Pi, C. Shao, C. Hu and H. Zhang, *J. Energy Inst.*, 2018, **91**, 733–742.
23 M. J. Boyd, A. A. Latimer, C. F. Dickens, A. C. Nielander, C. Hahn, J. K. Nørskov, D. C. Higgins and T. F. Jaramillo, *ACS Catal.*, 2019, **9**, 7578–7587.
24 J. H. Luo, Z. S. Hong, T. H. Chao and M. J. Cheng, *J. Phys. Chem. C*, 2019, **123**, 19033–19044.
25 H. Fei, J. Dong, Y. Feng, C. S. Allen, C. Wan, B. Volosskiy, M. Li, Z. Zhao, Y. Wang, H. Sun, P. An, W. Chen, Z. Guo, C. Lee, D. Chen, I. Shakir, M. Liu, T. Hu, Y. Li, A. I. Kirkland, X. Duan and Y. Huang, *Nat. Catal.*, 2018, **1**, 63–72.
26 C. Lei, H. Chen, J. Cao, J. Yang, M. Qiu, Y. Xia, C. Yuan, B. Yang, Z. Li, X. Zhang, L. Lei, J. Abbott, Y. Zhong, X. Xia, G. Wu, Q. He and Y. Hou, *Adv. Energy Mater.*, 2018, **8**, 1801912.
27 B. Lee and T. Hibino, *J. Catal.*, 2011, **279**, 233–240.
28 R. S. Rocha, R. M. Reis, M. R. V. Lanza and R. Bertazzoli, *Electrochim. Acta*, 2013, **87**, 606–610.
29 A. Tomita, J. Nakajima and T. Hibino, *Angew. Chem., Int. Ed.*, 2008, **47**, 1462–1464.
30 B. Lee, Y. Sakamoto, D. Hirabayashi, K. Suzuki and T. Hibino, *J. Catal.*, 2010, **271**, 195–200.
31 E. Perry Murray, T. Tsai and S. A. Barnett, *Nature*, 1999, **400**, 649–651.
32 S. Park, J. M. Vohs and R. J. Gorte, *Nature*, 2000, **404**, 265–267.
33 A. Torabi, J. Barton, C. Willman, H. Ghezel-Ayagh, N. Li, A. Poozhikunnath, R. Maric and O. Marina, *ECS Trans.*, 2016, **72**, 193–199.
34 S. Mukhopadhyay and A. T. Bell, *J. Mol. Catal. A: Chem.*, 2004, **211**, 59–65.
35 T. R. Cundari and A. Yoshikawa, *J. Comput. Chem.*, 1998, **19**, 902–911.
36 R. A. Periana, D. J. Taube, E. R. Evitt, D. G. Löffler, P. R. Wentrcek, G. Voss and T. Masuda, *Science*, 1993, **259**, 340–343.
37 M. E. O'Reilly, R. S. Kim, S. Oh and Y. Surendranath, *ACS Cent. Sci.*, 2017, **3**, 1174–1179.
38 N. Agarwal, S. J. Freakley, R. U. McVicker, S. M. Althahban, N. Dimitratos, Q. He, D. J. Morgan, R. L. Jenkins, D. J. Willock, S. H. Taylor, C. J. Kiely and G. J. Hutchings, *Science*, 2017, **358**, 223–227.
39 Y. Kwon, T. Y. Kim, G. Kwon, J. Yi and H. Lee, *J. Am. Chem. Soc.*, 2017, **139**, 17694–17699.
40 W. Huang, S. Zhang, Y. Tang, Y. Li, L. Nguyen, Y. Li, J. Shan, D. Xiao, R. Gagne, A. I. Frenkel and F. F. Tao, *Angew. Chem., Int. Ed.*, 2016, **55**, 13441–13445.
41 C. Hammond, M. M. Forde, M. H. Ab Rahim, A. Thetford, Q. He, R. L. Jenkins, N. Dimitratos, J. A. Lopez-Sanchez, N. F. Dummer, D. M. Murphy, A. F. Carley, S. H. Taylor, D. J. Willock, E. E. Stangland, J. Kang, H. Hagen, C. J. Kiely and G. J. Hutchings, *Angew. Chem., Int. Ed.*, 2012, **51**, 5129–5133.
42 D. Y. Osadchii, A. I. Olivos-Suarez, Á. Szécsényi, G. Li, M. A. Nasalevich, I. A. Dugulan, P. S. Crespo,

E. J. M. Hensen, S. L. Veber, M. V. Fedin, G. Sankar, E. A. Pidko and J. Gascon, *ACS Catal.*, 2018, **8**, 5542–5548.
43 S. Murcia-López, K. Villa, T. Andreu and J. R. Morante, *Chem. Commun.*, 2015, **51**, 7249–7252.
44 J. Xie, R. Jin, A. Li, Y. Bi, Q. Ruan, Y. Deng, Y. Zhang, S. Yao, G. Sankar, D. Ma and J. Tang, *Nat. Catal.*, 2018, **1**, 889–896.
45 X. Cui, H. Li, Y. Wang, Y. Hu, L. Hua, H. Li, X. Han, Q. Liu, F. Yang, L. He, X. Chen, Q. Li, J. Xiao, D. Deng and X. Bao, *Chem*, 2018, **4**, 1902–1910.
46 N. Spinner and W. E. Mustain, *J. Electrochem. Soc.*, 2013, **160**, F1275–F1281.
47 M. C. L. Santos, L. C. Nunes, L. M. G. Silva, A. S. Ramos, F. C. Fonseca, R. F. B. de Souza and A. O. Neto, *ChemistrySelect*, 2019, **4**, 11430–11434.
48 M. Ma, B. J. Jin, P. Li, M. S. Jung, J. Il Kim, Y. Cho, S. Kim, J. H. Moon and J. H. Park, *Adv. Sci.*, 2017, **4**, 1700379.
49 N. Spinner and W. E. Mustain, *J. Electrochem. Soc.*, 2013, **160**, 1275–1281.
50 Y. Amenomiya, V. I. Birss, M. Goledzinowski, J. Galuszka and A. R. Sanger, *Catal. Rev.*, 1990, **32**, 163–227.
51 Z. Y. Ma, C. Yang, W. Wei, W. H. Li and Y. H. Sun, *J. Mol. Catal. A: Chem.*, 2005, **227**, 119–124.
52 H. Ahn and T. J. Marks, *J. Am. Chem. Soc.*, 1999, **120**, 13533–13534.
53 B. Samaranch, P. Ramírez de la Piscina, G. Clet, M. Houalla, P. Gélin and N. Homs, *Chem. Mater.*, 2007, **19**, 1445–1451.
54 M. Ma, C. Oh, J. Kim, J. H. Moon and J. H. Park, *Appl. Catal., B*, 2019, **259**, 118095.
55 F. M. Pinto, V. Y. Suzuki, R. C. Silva and F. A. La Porta, *Front. Mater.*, 2019, **6**, 260.
56 R. A. Van Santen, I. Tranca and E. J. M. Hensen, *Catal. Today*, 2015, **244**, 63–84.
57 Z. F. Pan, L. An, T. S. Zhao and Z. K. Tang, *Prog. Energy Combust. Sci.*, 2018, **66**, 141–175.
58 R. S. Rocha, L. M. Camargo, M. R. V. Lanza and R. Bertazzoli, *Electrocatalysis*, 2010, **1**, 224–229.
59 N. Spinner and W. E. Mustain, *Electrochim. Acta*, 2011, **56**, 5656–5666.
60 N. S. Spinner, J. A. Vega and W. E. Mustain, *Catal. Sci. Technol.*, 2012, **2**, 19–28.
61 J. A. Labinger and J. E. Bercaw, *J. Organomet. Chem.*, 2015, **793**, 47–53.
62 Y. Chen, B. DeGlee, Y. Tang, Z. Wang, B. Zhao, Y. Wei, L. Zhang, S. Yoo, K. Pei, J. H. Kim, Y. Ding, P. Hu, F. F. Tao and M. Liu, *Nat. Energy*, 2018, **3**, 1042–1050.
63 W. Li, D. He, G. Hu, X. Li, G. Banerjee, J. Li, S. H. Lee, Q. Dong, T. Gao, G. W. Brudvig, M. M. Waegele, D. E. Jiang and D. Wang, *ACS Cent. Sci.*, 2018, **4**, 631–637.
64 K. W. Frese, *Langmuir*, 1991, **7**, 13–15.
65 T. J. Omasta, W. A. Rigdon, C. A. Lewis, R. J. Stanis, R. Liu, C. Q. Fan and W. E. Mustain, *ECS Trans.*, 2015, **66**, 129–136.
66 M. Safariamin, L. H. Tidahy, E. Abi-Aad, S. Siffert and A. Aboukaïs, *C. R. Chim.*, 2009, **12**, 748–753.
67 S. Zhang, S. Muratsugu, N. Ishiguro and M. Tada, *ACS Catal.*, 2013, **3**, 1855–1864.
68 A. Kambolis, H. Matralis, A. Trovarelli and C. Papadopoulou, *Appl. Catal., A*, 2010, **377**, 16–26.
69 K. Hashimoto, S. Watase and N. Toukai, *Catal. Lett.*, 2002, **80**, 147–152.
70 A. R. Derk, G. M. Moore, S. Sharma, E. W. McFarland and H. Metiu, *Top. Catal.*, 2014, **57**, 118–124.
71 C. Zhu, S. Hou, X. Hu, J. Lu, F. Chen and K. Xie, *Nat. Commun.*, 2019, **10**, 1–8.
72 J. Lu, C. Zhu, C. Pan, W. Lin, J. P. Lemmon, F. Chen, C. Li and K. Xie, *Sci. Adv.*, 2018, **4**, eaar5100.
73 V. Sariboğa and F. Öksüzömer, *Appl. Energy*, 2012, **93**, 707–721.
74 T. Liu, H. Liu, X. Zhang, L. Lei, Y. Zhang, Z. Yuan, F. Chen and Y. Wang, *J. Mater. Chem. A*, 2019, **7**, 13550–13558.
75 M. Farnak, J. A. Esfahani and S. Bozorgmehri, *Renewable Energy*, 2020, **147**, 155–163.
76 S. B. Adler, *Chem. Rev.*, 2004, **104**, 4791–4843.
77 J. Tong, D. Clark, M. Hoban and R. O'Hayre, *Solid State Ionics*, 2010, **181**, 496–503.
78 D. Pergolesi, E. Fabbri, A. D'Epifanio, E. Di Bartolomeo, A. Tebano, S. Sanna, S. Licoccia, G. Balestrino and E. Traversa, *Nat. Mater.*, 2010, **9**, 846–852.
79 Y. Yamazaki, R. Hernandez-Sanchez and S. M. Haile, *Chem. Mater.*, 2009, **21**, 2755–2762.
80 P. Babilo and S. M. Haile, *J. Am. Ceram. Soc.*, 2005, **88**, 2362–2368.
81 C. Duan, J. Tong, M. Shang, S. Nikodemski, M. Sanders, S. Ricote, A. Almansoori and R. O'Hayre, *Science*, 2015, **349**, 1321–1326.
82 D. Zagoraios, A. Athanasiadi, I. Kalaitzidou, S. Ntais, A. Katsaounis, A. Caravaca, P. Vernoux and C. G. Vayenas, *Catal. Today*, 2019, DOI: 10.1016/j.cattod.2019.02.030.
83 C. G. Vayenas and S. Brosda, *Top. Catal.*, 2014, **57**, 1287–1301.
84 M. Y. Sinev, Y. P. Tulenin, O. V. Kalashnikova, V. Y. Bychkov and V. N. Korchak, *Catal. Today*, 1996, **32**, 157–162.
85 J. C. Forti, R. S. Rocha, M. R. V. Lanza and R. Bertazzoli, *J. Electroanal. Chem.*, 2007, **601**, 63–67.
86 S. H. Morejudo, R. Zanón, S. Escolástico, I. Yuste-Tirados, H. Malerød-Fjeld, P. K. Vestre, W. G. Coors, A. Martínez, T. Norby, J. M. Serra and C. Kjølseth, *Science*, 2016, **353**, 563–566.
87 H. Xu, B. Chen, J. Irvine and M. Ni, *Int. J. Hydrogen Energy*, 2016, **41**, 21839–21849.
88 C. Duan, R. Kee, H. Zhu, N. Sullivan, L. Zhu, L. Bian, D. Jennings and R. O'Hayre, *Nat. Energy*, 2019, **4**, 230–240.
89 B. J. M. Sarruf, J. E. Hong, R. Steinberger-Wilckens and P. E. V. de Miranda, *Int. J. Hydrogen Energy*, 2020, **45**, 5297–5308.
90 K. D. Kreuer, *Solid State Ionics*, 1999, **125**, 285–302.
91 T. Ikuno, J. Zheng, A. Vjunov, M. Sanchez-Sanchez, M. A. Ortuño, D. R. Pahls, J. L. Fulton, D. M. Camaioni, Z. Li, D. Ray, B. L. Mehdi, N. D. Browning, O. K. Farha, J. T. Hupp, C. J. Cramer, L. Gagliardi and J. A. Lercher, *J. Am. Chem. Soc.*, 2017, **139**, 10294–10301.
92 S. I. Chan, Y. J. Lu, P. Nagababu, S. Maji, M. C. Hung, M. M. Lee, I. J. Hsu, P. D. Minh, J. C. H. Lai, K. Y. Ng, S. Ramalingam, S. S. F. Yu and M. K. Chan, *Angew. Chem., Int. Ed.*, 2013, **52**, 3731–3735.

